# **Supporting Information**

# Mechanical bonds in polymer backbones: Does more mean better?

Jianzhen Wu, Guoquan Liu, Yi Ding, Wenbin Wang, Arslan Muhammad, Zhaoming Zhang\*, Xuzhou Yan\*

State Key Laboratory of Synergistic Chem-Bio Synthesis, Frontiers Science Center for Transformative Molecules, School of Chemistry and Chemical Engineering, Shanghai Jiao Tong University, Shanghai 200240, P. R.

\*Correspondence to: zhangzhaoming@sjtu.edu.cn; xzyan@sjtu.edu.cn

# **Contents**

1.Materials and general methods	S3		
2. Syntheses of [2]rotaxane	S16S20S21S22S22S24		
		References	S34

### 1.Materials and general methods

All reagents were commercially available and used as supplied without further purification. Deuterated solvents were purchased from Cambridge Isotope Laboratory (Andover, MA). All reactions were performed at ambient laboratory conditions, and no precautions were taken to exclude atmospheric moisture unless otherwise specified. Compounds 1–8 and [2]rotaxane were all prepared according to the established methods.<sup>[1,2]</sup>

Nuclear magnetic resonance (NMR) spectra were recorded with a Bruker Avance DMX 400 spectrophotometer with use of the deuterated solvent as the lock and the residual solvent or TMS as the internal reference. <sup>1</sup>H NMR chemical shifts are reported relative to residual solvent signals. Fourier transform infrared (FT-IR) spectroscopy was performed on a Thermoscientific Nicolet 6700 FT-IR spectrometer at room temperature in the range of 500~4000 cm<sup>-1</sup>. The thermal stability analysis was conducted using a TA Instruments Q500 thermogravimetric analyzer (TGA) under the nitrogen. Each sample (~8 mg) was heated from 50 to 800 °C with a rate of 20 °C/min. Transition temperatures of materials were determined on a TA Instruments 2500 differential scanning calorimetry (DSC) under the nitrogen. Each sample (~10 mg) was analyzed by utilizing a heat/cool/heat cycle with a heating or cooling rate of 20 °C/min. Dynamic mechanical analyses (DMA) were performed on Discovery DMA Q850 apparatus (Germany) with a tensile mode. The creep-recovery tests were carried out with an automatic tension setting of 125%.

*Tensile tests:* The mechanical properties of the samples were measured using an Instron 3343 machine in standard stress—strain experiments. Unless otherwise noted, the tensile stress was measured at a constant speed of 100 mm/min. The determination of each curve was repeated five times to avoid any accidental error. The toughness, a parameter that characterizes the work required to fracture the sample per unit, was calculated from the area below the tension stress—strain curve until fracture.

Puncture resistance tests: The samples were fixed between two plates with a distance of 5 mm to let the samples deform freely during the test. The as-prepared samples were cut into 5 mm (width) × 15 mm (length) × 0.3 mm (thickness) rectangles for the puncture resistance measurements. A toothpick was positioned perpendicularly and moved down to the sample in a tensile test instrument with a speed at 50 mm/min. The puncture resistance was evaluated by maximal puncture force and displacement. The puncture energy was obtained by integrating the area under puncture force—displacement curve.

**Swelling tests:** The swelling experiments were performed with a piece of sample (~20 mg). The samples were immersed in different kinds of solvents for about 3 hours at room temperature. The swelling ratio was calculated by:

Swelling ratio 
$$(g/g) = (m_1 - m_2)/m_2$$

where  $m_1$  and  $m_2$  are the weights of the swollen and dry sample, respectively.

**Rheological test:** Rheological experiments were carried out using a TA Instruments ARES G2 strain-controlled rheometer with an 8 mm parallel plate attachment. The asprepared samples were cut into circles with a radius of 4 mm for the rheological measurements.

Procedure for the preparation of the PNs: Taking the preparation of PN-3 as an example, [2]rotaxane together with the cross-linker PETMP were firstly dissolved in THF solution at a molar ratio of 2:1. The blended solution was then molded and exposed to the UV light (365 nm) to induce the thiol-ene click reaction by photoinitiation. Afterwards, the networks were put in an oven at 65 °C for 12 h to further cure the samples. Following the steps above, PN-2 and PN-1 were prepared in the same way by replacing half and all of the [2]rotaxane with bis(2-vinyloxyethyl) ether monomer, respectively, in the blended solution.

Additional control networks (PNs-4-9) were similarly prepared by replacing the

comonomer bis(2-vinyloxyethyl) ether with the longer monomers (monomer C and monomer D), or by substituting the [2]rotaxane with its acetylated, charge-free analogue (monomer E), while keeping all other reaction conditions identical, including molar ratios, solvent, UV irradiation protocol, and thermal curing steps.

## 2. Syntheses of [2]rotaxane

# Host

## Guest

## [2]rotaxane

4

$$H_2$$
 $H_2$ 
 $H_2$ 

**Scheme S1.** Synthetic routes to [2]rotaxane.

A mixture of methyl 3,4-dihydroxybenzoate (5.3 g, 31.5 mmol),  $K_2CO_3$  (8.7 g, 63.1 mmol),  $KPF_6$  (8.7 g, 47.3 mmol) and compound **1** (20.0 g, 31.5 mmol) in 200 mL of  $CH_3CN$  was stirred and heated for two days under  $N_2$  protection. After cooling, the mixture was filtered and  $CH_3CN$  was removed with a rotary evaporator, and then  $CH_2Cl_2$  was added. After washing with water several times, the organic phase was dried with  $Na_2SO_4$  and then concentrated. The residue was purified by flash column chromatography ( $CH_2Cl_2/CH_3OH$ , 30:1 v/v) to afford compound **2** (6.4 g, 44%) as a pale yellow oil. The <sup>1</sup>H NMR spectrum of compound **2** is shown in Figure S1. <sup>1</sup>H NMR (400 MHz,  $CDCl_3$ , 298K)  $\delta$  (ppm): 7.60 (dd, J = 8, 2 Hz, 1H), 7.50 (d, J = 2 Hz, 1H), 6.83 (d, J = 9 Hz, 1H), 4.16 (ddd, J = 6, 3, 2 Hz, 4H), 3.91–3.86 (m, 4H), 3.83 (s, 3H), 3.75 (ddd, J = 6, 3, 1 Hz, 4H), 3.69–3.58 (m, 16H).

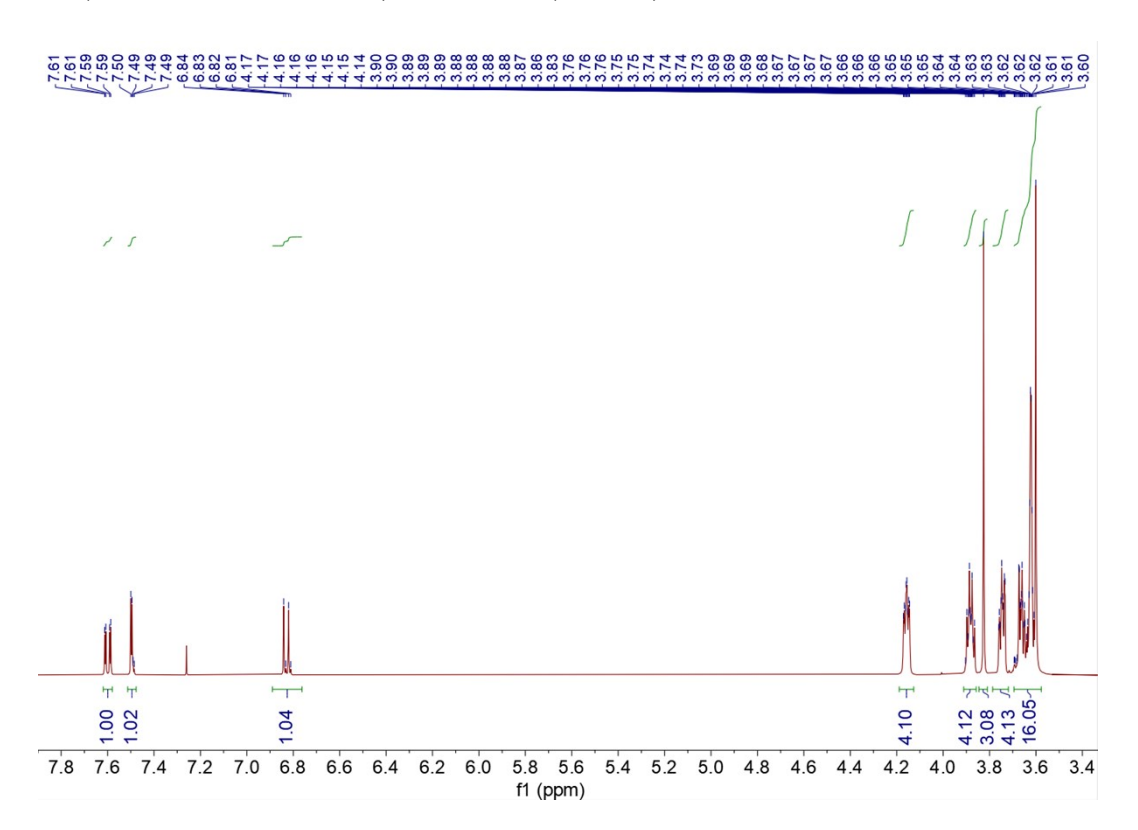


Figure S1. <sup>1</sup>H NMR spectrum (400 MHz, CDCl<sub>3</sub>, 298K) of compound 2.

To a solution of compound **2** (6.4 g, 13.9 mmol) in CH<sub>3</sub>OH (20 mL) and THF (40 mL) was added aqueous NaOH solution (1.2 M, 30 mL). The solution was then heated and stirred for 12 h. Upon cooling to room temperature, HCl was added to pH = 4. The solution was concentrated and the resulting residue was washed with water thoroughly and dried to afford compound **3** (6.2 g, 99%) as a yellow oil. The <sup>1</sup>H NMR spectrum of compound **3** is shown in Figure S2. <sup>1</sup>H NMR (400 MHz, CDCl<sub>3</sub>, 298K)  $\delta$  (ppm): 7.70 (dd, J = 8, 2 Hz, 1H), 7.57 (d, J = 2 Hz, 1H), 6.88 (d, J = 9 Hz, 1H), 4.21 (td, J = 6, 4 Hz, 4H), 3.98–3.90 (m, 4H), 3.80 (ddd, J = 6, 3, 2 Hz, 4H), 3.74–3.61 (m, 16H).

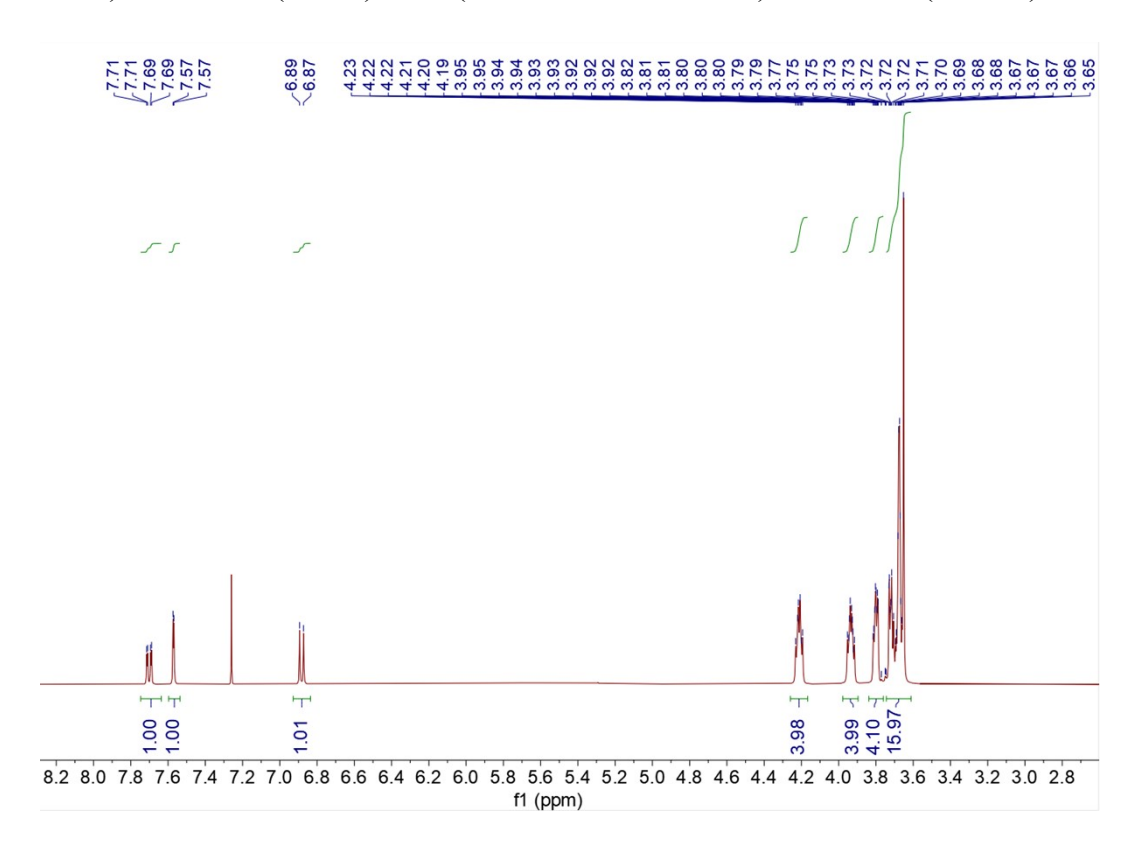


Figure S2. <sup>1</sup>H NMR spectrum (400 MHz, CDCl<sub>3</sub>, 298K) of compound 3.

To a solution of compound **3** (10.0 g, 22.5 mmol) and 10-bromo-1-decene (7.4 g, 33.8 mmol) in CH<sub>3</sub>CN (100 mL), K<sub>2</sub>CO<sub>3</sub> (6.2 g, 45.0 mmol) was added at room temperature. The mixture was heated to 85 °C and stirred for 20 h. The reaction mixture was cooled to room temperature and filtered, then concentrated to afford a yellow oil. The product was purified by flash column chromatography (CH<sub>2</sub>Cl<sub>2</sub>/MeOH, 30:1 v/v) to afford compound **4** as a pale yellow oil (11.2 g, 85%). The <sup>1</sup>H NMR spectrum of compound **4** is shown in Figure S3. <sup>1</sup>H NMR (400 MHz, CDCl<sub>3</sub>, 298K)  $\delta$  (ppm): 7.63 (dd, J = 8, 2 Hz, 1H), 7.53 (d, 1H), 6.85 (d, J = 8 Hz, 1H), 5.83–5.73 (m, 1H), 5.00–4.89 (m, 2H), 4.27–4.23 (m, 2H), 4.20–4.18 (m, 4H), 3.92–3.89 (m, 4H), 3.79–3.63 (m, 20H), 2.05–1.99 (m, 2H), 1.76–1.71 (m, 2H), 1.44–1.23 (m, 10H).

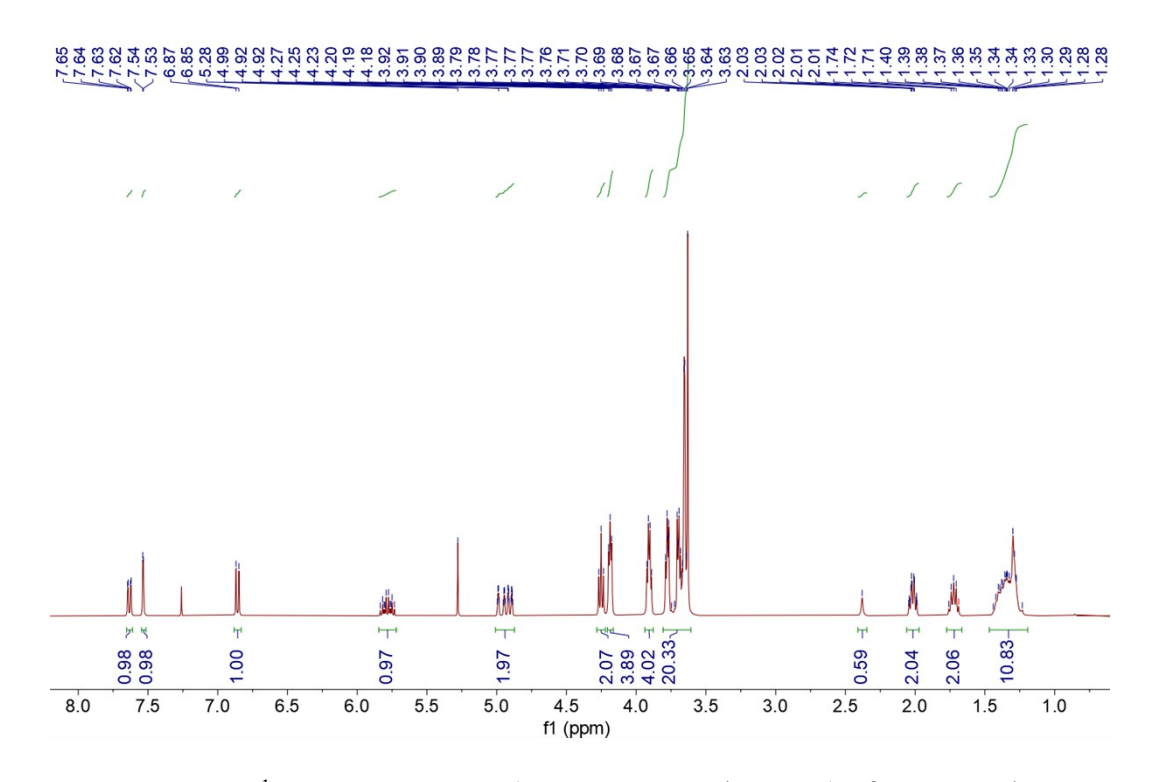


Figure S3. <sup>1</sup>H NMR spectrum (400 MHz, CDCl<sub>3</sub>, 298K) of compound 4.

A solution of 3,5-dimethyl-4-hydroxybenzaldehyde (6.9 g, 46.2 mmol) and compound **5** (8.0 g, 46.2 mmol) was refluxed overnight in CH<sub>3</sub>OH (200 mL). After the reaction, mixture was cooled to ambient temperature, NaBH<sub>4</sub> (3.5 g, 92.4 mmol) was added to the stirring solution over a period of 30 min. Stirring was maintained under ambient conditions for further 24 h, after which H<sub>2</sub>O was added to neutralize excess NaBH<sub>4</sub>. The mixture was filtered and CH<sub>3</sub>OH was removed with a rotary evaporator. The residue was extracted with CH<sub>2</sub>Cl<sub>2</sub>, and di-tert-butyl decarbonate (12.1 g, 55.4 mmol) was added to the organic phase and stirred for 12 h. The product was purified by flash column chromatography (petroleum ether/ethyl acetate, 10:1 v/v) to afford compound **6** as a red oil (8.7 g, 46%). The <sup>1</sup>H NMR spectrum of compound **6** is shown in Figure S4. <sup>1</sup>H NMR (400 MHz, CDCl<sub>3</sub>, 298K)  $\delta$  (ppm): 6.81 (s, 2H), 4.27 (s, 2H), 3.62 (t, J = 7 Hz, 2H), 3.23–2.98 (m, 3H), 2.21 (s, 6H), 1.59–1.37 (m, 16H), 1.36–1.17 (m, 15H).

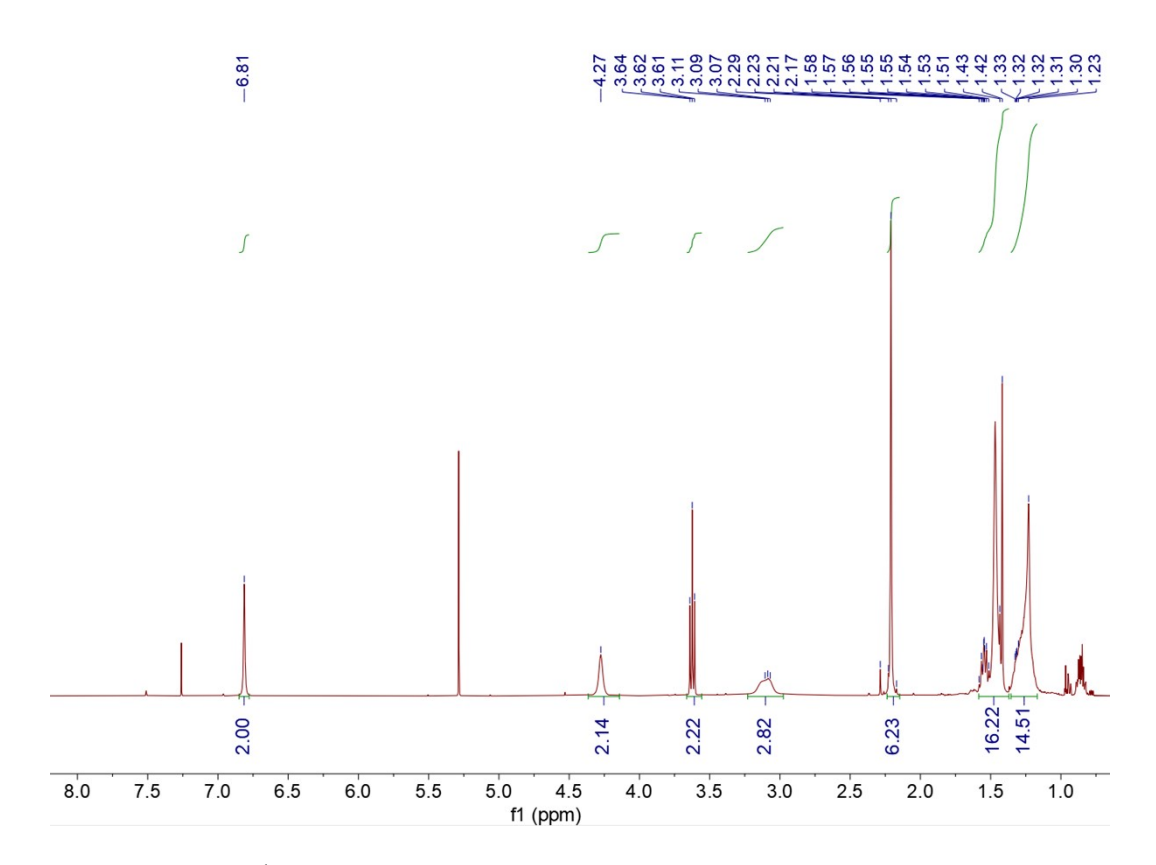


Figure S4.  $^1\text{H}$  NMR spectrum (400 MHz, CDCl $_3$ , 298K) of compound 6.

To a solution of compound **6** (5.0 g, 12.3 mmol) and 10-bromo-1-decene (4.0 g, 18.5 mmol) in CH<sub>3</sub>CN (120 mL), K<sub>2</sub>CO<sub>3</sub> (3.4 g, 24.5 mmol) was added at room temperature. The stirred mixture was heated at 65 °C for 12 h. The reaction mixture was cooled to room temperature and filtered, and concentrated to give a yellow oil, which was purified by flash column chromatography (CH<sub>2</sub>Cl<sub>2</sub>/ethyl acetate, 30:1 v/v) to afford compound 7 as a yellow oil (3.0 g, 45%). The <sup>1</sup>H NMR spectrum of compound 7 is shown in Figure S5. <sup>1</sup>H NMR (400 MHz, CDCl<sub>3</sub>, 298K)  $\delta$  (ppm): 6.83 (s, 2H), 5.85–5.73 (m, 1H), 5.01–4.88 (m, 2H), 4.29 (d, J = 4 Hz, 2H), 4.10 (q, J = 7 Hz, 1H), 3.71 (t, J = 7 Hz, 2H), 3.61 (t, J = 7 Hz, 2H), 3.11 (s, 2H), 2.23 (s, 6H), 2.08–1.98 (m, 4H), 1.78 (td, J = 15, 6 Hz, 3H), 1.57–1.15 (m, 38H).

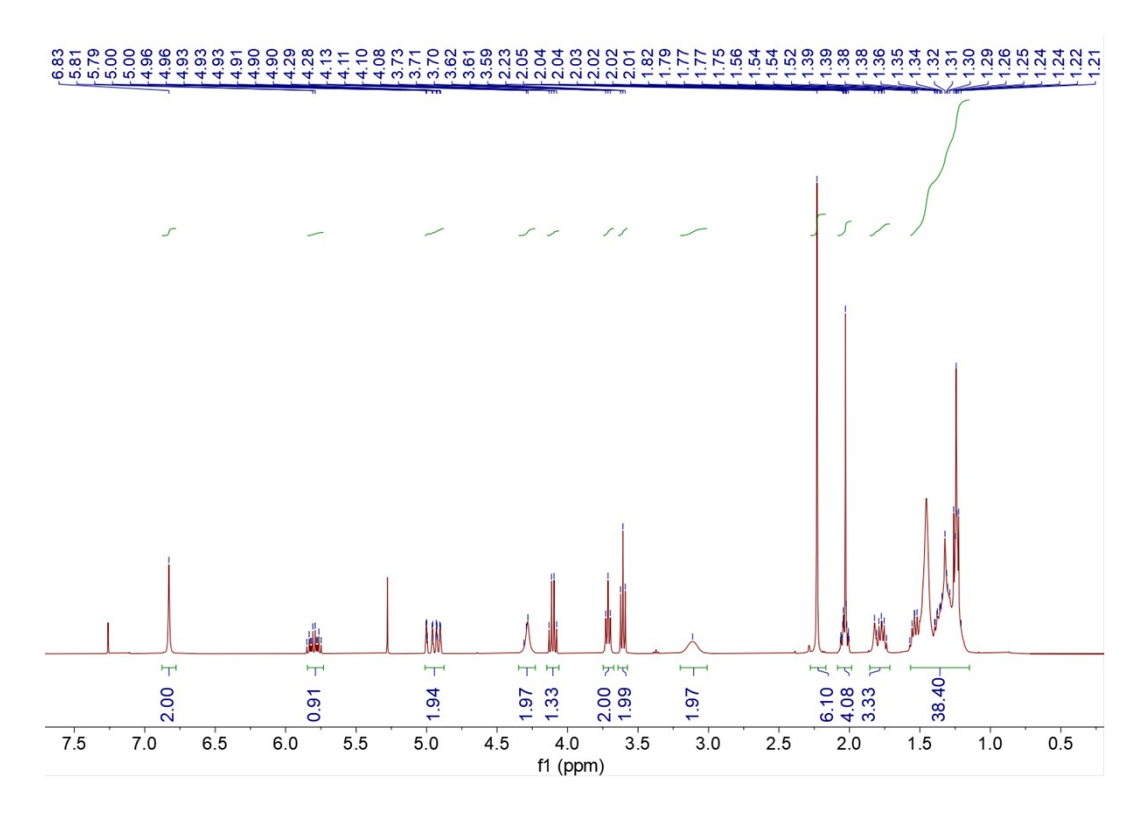


Figure S5. <sup>1</sup>H NMR spectrum (400 MHz, CDCl<sub>3</sub>, 298K) of compound 7.

The solution of compound 7 (3.0 g, 5.5 mmol) as a yellow oil was added to a hydrochloric acid solution and stirred for 12 h at room temperature. White precipitate formed during this procedure. The mixture was extracted first to remove all the acid. All the solvents were then evaporated. The solid left was dissolved in acetone and the solution was added to a saturated aqueous NH<sub>4</sub>PF<sub>6</sub> solution, producing a new precipitate. The precipitate was then collected by suction filtration to afford compound 8 (3.1 g, 96%) as a white solid. The <sup>1</sup>H NMR spectrum of compound 8 is shown in Figure S6. <sup>1</sup>H NMR (400 MHz, CDCl<sub>3</sub>, 298K)  $\delta$  (ppm): 7.14 (s, 2H), 5.78 (ddt, J = 17, 10, 7 Hz, 1H), 4.99–4.85 (m, 2H), 3.89 (s, 2H), 3.63 (t, J = 7 Hz, 2H), 3.54 (t, J = 7 Hz, 2H), 2.80–2.66 (m, 2H), 2.21 (s, 6H), 2.01 (q, J = 7 Hz, 2H), 1.74 (dt, J = 15, 6 Hz, 4H), 1.51–1.41 (m, 4H), 1.41–1.14 (m, 20H).

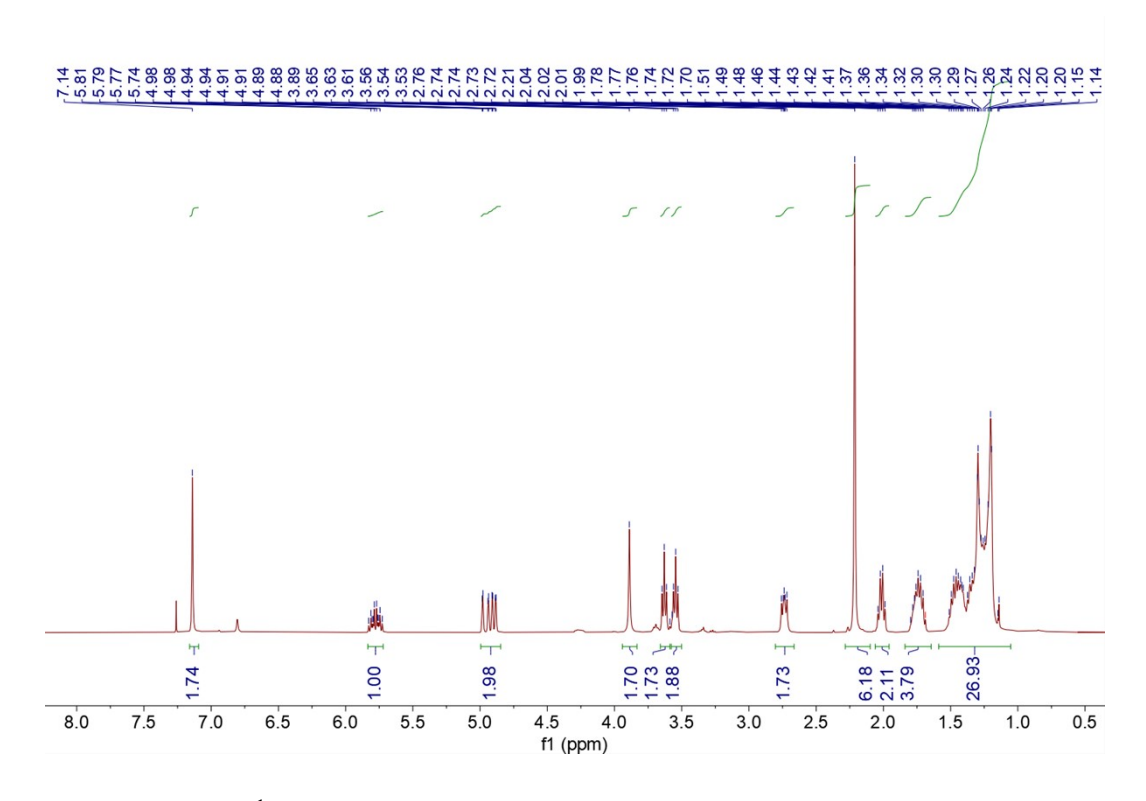


Figure S6. <sup>1</sup>H NMR spectrum (400 MHz, CDCl<sub>3</sub>, 298K) of compound 8.

#### Synthesis of [2]rotaxane

4

$$A_{p}$$
 $A_{p}$ 
 $A_{p}$ 

A stirred solution of compounds **4** (1.0 g, 1.7 mmol) and **8** (1.0 g, 1.7 mmol) in dry  $CH_2Cl_2$  (60 mL) in a round-bottomed flask with a magnetic stir-bar was heated to reflux for 48 h under  $N_2$ . Upon cooling to room temperature, 3,5-dimethylphenyl isocyanate (0.5 g, 3.4 mmol) and 0.1 mL of dibutyltin dilaurate were added to the solution which was stirred at room temperature for another 12 h. The solution was evaporated and the residue was purified by gel chromatography ( $CH_2Cl_2$ /acetone, 50:1 v/v) to afford [2]rotaxane as a yellow oil (1.3 g, 63%). The <sup>1</sup>H NMR spectrum of [2]rotaxane is shown in Figure S7. <sup>1</sup>H NMR (400 MHz, CDCl<sub>3</sub>, 298K)  $\delta$  (ppm): 7.63 (dd, J = 8, 2 Hz, 1H), 7.47 (d, J = 2 Hz, 1H), 7.06–6.97 (m, 6H), 6.86 (d, J = 8 Hz, 1H), 6.69 (s, 1H), 5.87–5.73 (m, 2H), 5.02–4.91 (m, 4H), 4.36 (t, J = 7 Hz, 2H), 4.27 (t, J = 7 Hz, 2H), 4.22–4.08 (m, 6H), 3.96–3.82 (m, 4H), 3.67–3.59 (m, 6H), 3.58–3.32 (m, 16H), 3.19–3.07 (m, 2H), 2.27 (s, 6H), 2.18 (s, 6H), 2.08–1.99 (m, 4H), 1.80–1.71 (m, 4H), 1.68–1.62 (m, 2H), 1.58–1.47 (m, 2H), 1.43–1.23 (m, 30H).

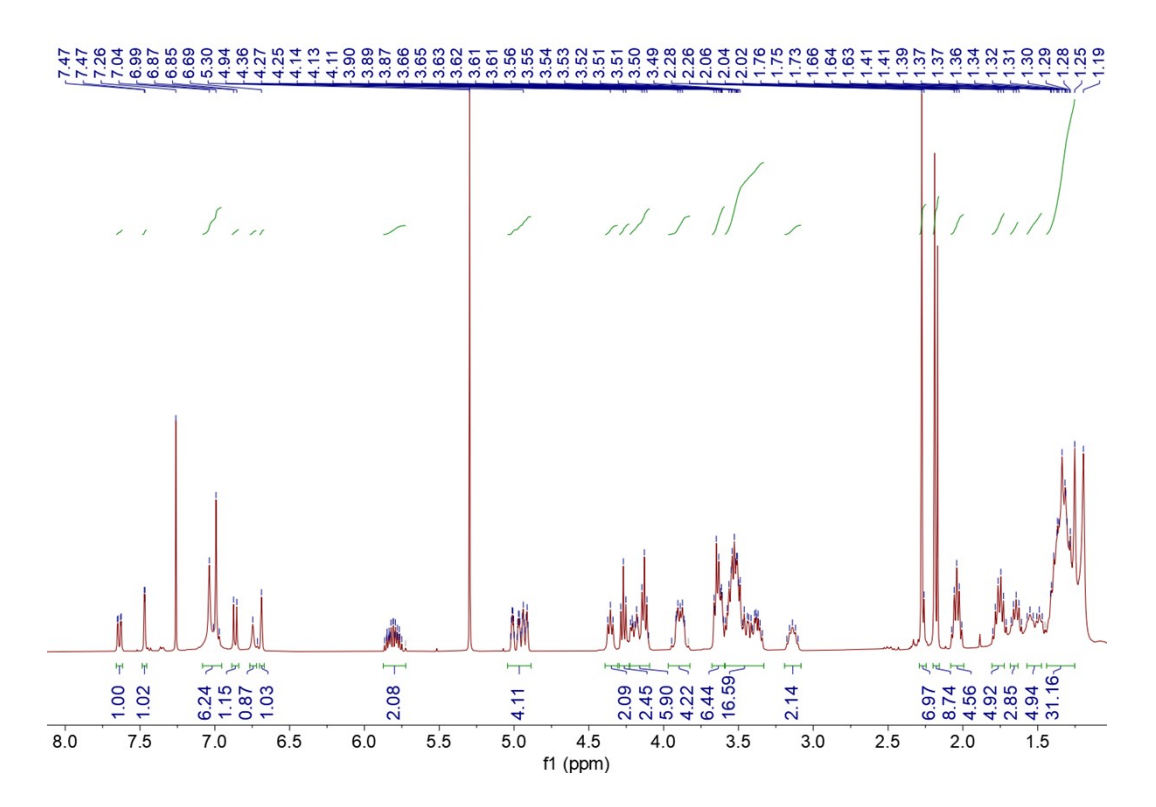


Figure S7. <sup>1</sup>H NMR spectrum (400 MHz, CDCl<sub>3</sub>, 298K) of [2]rotaxane.

#### 3. Syntheses of other important compounds

#### Synthesis of monomer C

To a solution of hexaethylene glycol (5.0 g, 17.7 mmol) and allyl bromide (6.4 g, 53.1 mmol) in DMF (25 mL), NaH (2.6 g, 108.3 mmol) was then added slowly. The mixture was stirred for 1 h at room temperature. The reaction was then carefully quenched by methanol and the mixture was diluted with brine. The product was extracted with ethyl acetate and then purified by flash column chromatography (petroleum ether/acetone, 3:1 v/v) to afford monomer C as pale yellow liquid (6.6 g, 98%). The <sup>1</sup>H NMR spectrum of monomer C is shown in Figure S8. <sup>1</sup>H NMR (400 MHz, CDCl<sub>3</sub>, 298K)  $\delta$  (ppm): 5.87 (ddt, J = 17, 10, 5 Hz, 2H), 5.26–5.11 (m, 4H), 3.98 (dt, J = 5, 1 Hz, 4H), 3.64–3.54 (m, 24H).

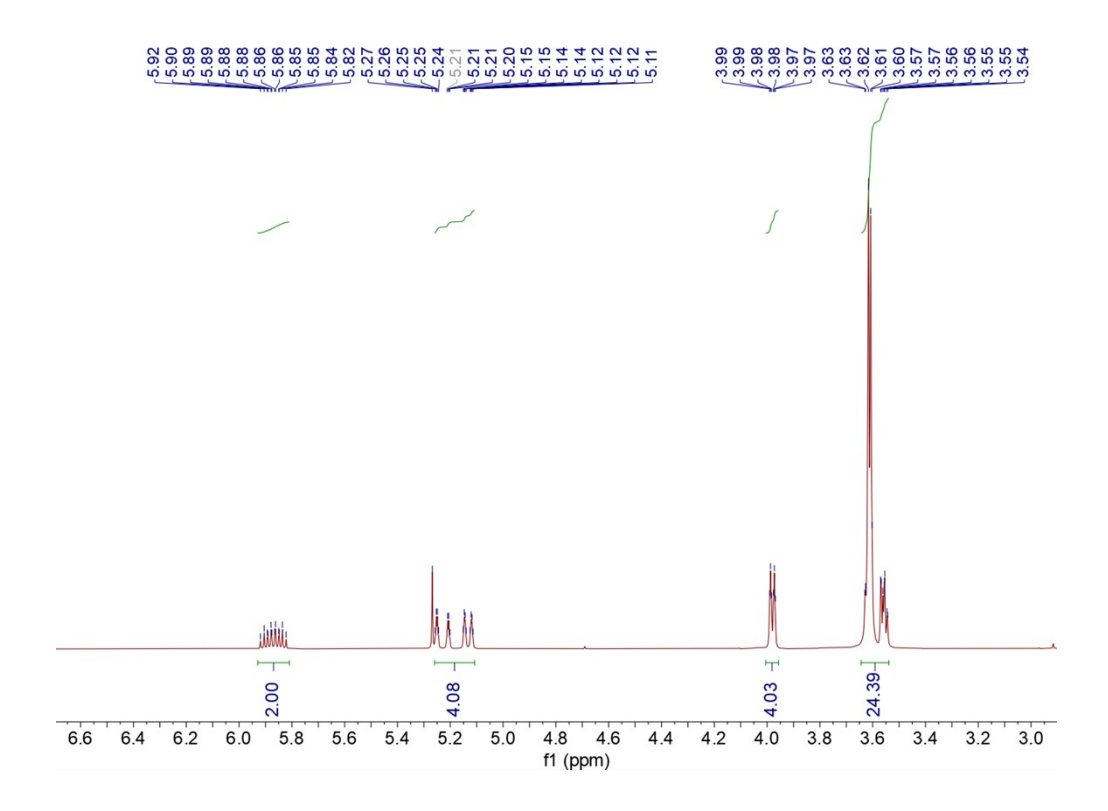


Figure S8. <sup>1</sup>H NMR spectrum (400 MHz, CDCl<sub>3</sub>, 298K) of monomer C.

#### Synthesis of monomer D

A solution of 1,4-benzenedicarboxylic acid (2.0 g, 12.0 mmol) and 9-hydroxy-1-decene (5.6 g, 36.0 mmol) was refluxed overnight in CH<sub>2</sub>Cl<sub>2</sub> (200 mL) with EDC.HCl (9.2 g, 48.0 mmol) and DMAP (1.3 g, 10.8 mmol) at room temperature. After the reaction, CH<sub>2</sub>Cl<sub>2</sub> was removed with a rotary evaporator. The product was purified by flash column chromatography (petroleum ether/ethyl acetate, 10:1 v/v) to afford monomer D as a white solid powder (4.3 g, 80%). The <sup>1</sup>H NMR spectrum of monomer D is shown in Figure S9. <sup>1</sup>H NMR (400 MHz, CDCl<sub>3</sub>, 298K)  $\delta$  (ppm): 8.09 (s, 4H), 5.81 (ddt, J = 16, 10, 6 Hz, 2H), 5.03–4.90 (m, 4H), 4.33 (t, J = 6 Hz, 4H), 2.04 (tdd, J = 6, 5, 1 Hz, 4H), 1.82–1.71 (m, 4H), 1.49–1.21 (m, 23H).

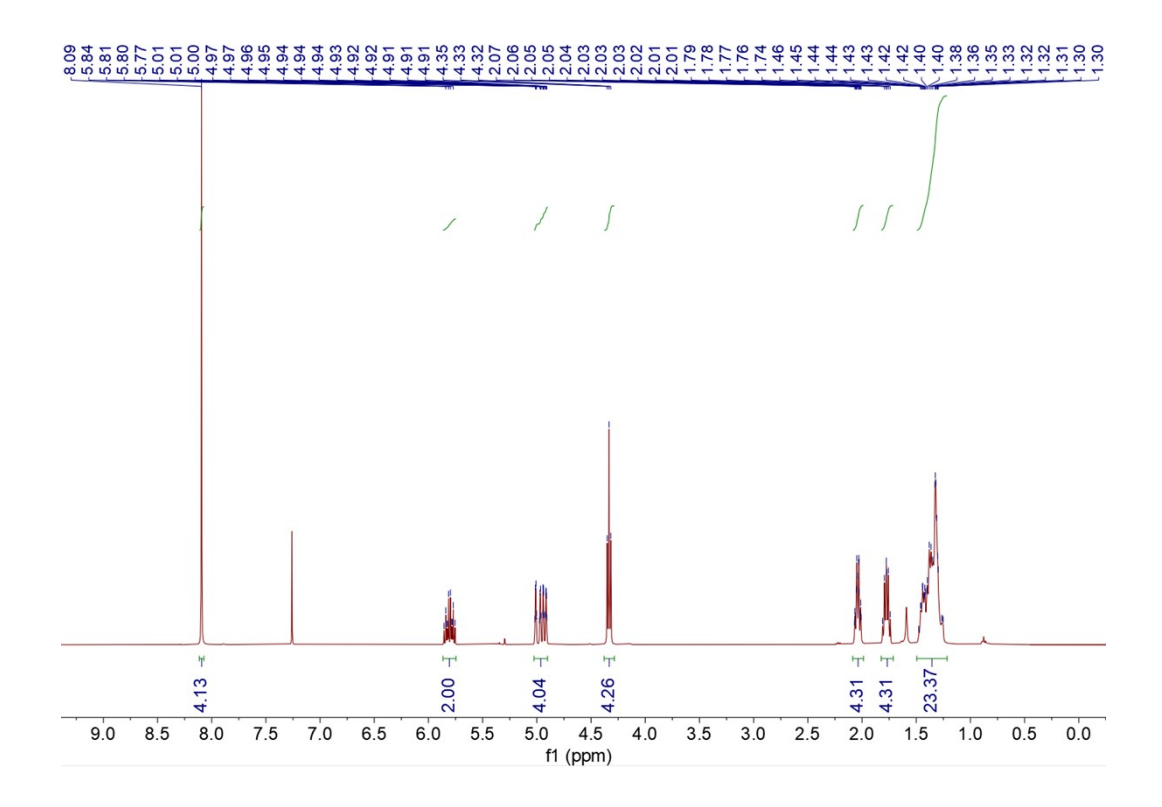


Figure S9. <sup>1</sup>H NMR spectrum (400 MHz, CDCl<sub>3</sub>, 298K) of monomer D.

#### Synthesis of monomer E

To a solution of [2]rotaxane (0.4 g, 0.3 mmol) and triethylamine (TEA) (0.4 g, 3.2 mmol) in dry THF (20 mL), acetic anhydride (0.2 g, 1.6 mmol) was added and then stirred for 24 h at 40 °C. The mixture was diluted with  $CH_2CI_2$  and washed with brine. Then, the solvent was removed under reduced pressure. The residue was purified by flash column chromatography ( $CH_2CI_2$ /acetone, 10:1 v/v) to afford monomer E as a pale yellow oil (0.3 g, 81%). The <sup>1</sup>H NMR spectrum of monomer E is shown in Figure S10. <sup>1</sup>H NMR (400 MHz, CDCI<sub>3</sub>, 298K)  $\delta$  (ppm): 7.61 (dd, J = 8, 2 Hz, 1H), 7.47 (t, J = 2 Hz, 1H), 7.17 (s, 2H), 6.85 (s, 1H), 6.81–6.76 (m, 2H), 6.55 (d, J = 4 Hz, 1H), 5.80 (dddd, J = 17, 10, 7, 4 Hz, 2H), 5.03–4.89 (m, 4H), 4.47 (s, 1H), 4.39 (s, 1H), 4.33–4.17 (m, 6H), 4.16–4.04 (m, 3H), 3.99 (dd, J = 9, 5 Hz, 2H), 3.83–3.76 (m, 2H), 3.75–3.60 (m, 10H), 3.60–3.46 (m, 12H), 3.35–3.27 (m, 1H), 3.15 (t, J = 8 Hz, 1H), 2.28–2.19 (m, 13H), 2.17 (s, 2H), 2.09 (s, 2H), 2.08–1.98 (m, 6H), 1.76 (ddt, J = 17, 14, 7 Hz, 5H), 1.63 (s, 14H), 1.51 (s, 7H), 1.44–1.23 (m, 38H). HRESIMS is shown in Figure S11: m/z calcd for  $C_{71}H_{112}N_2O_{14}$ , 1239.6770 [M + Na]+; found 1239.8015 [M + Na]+.

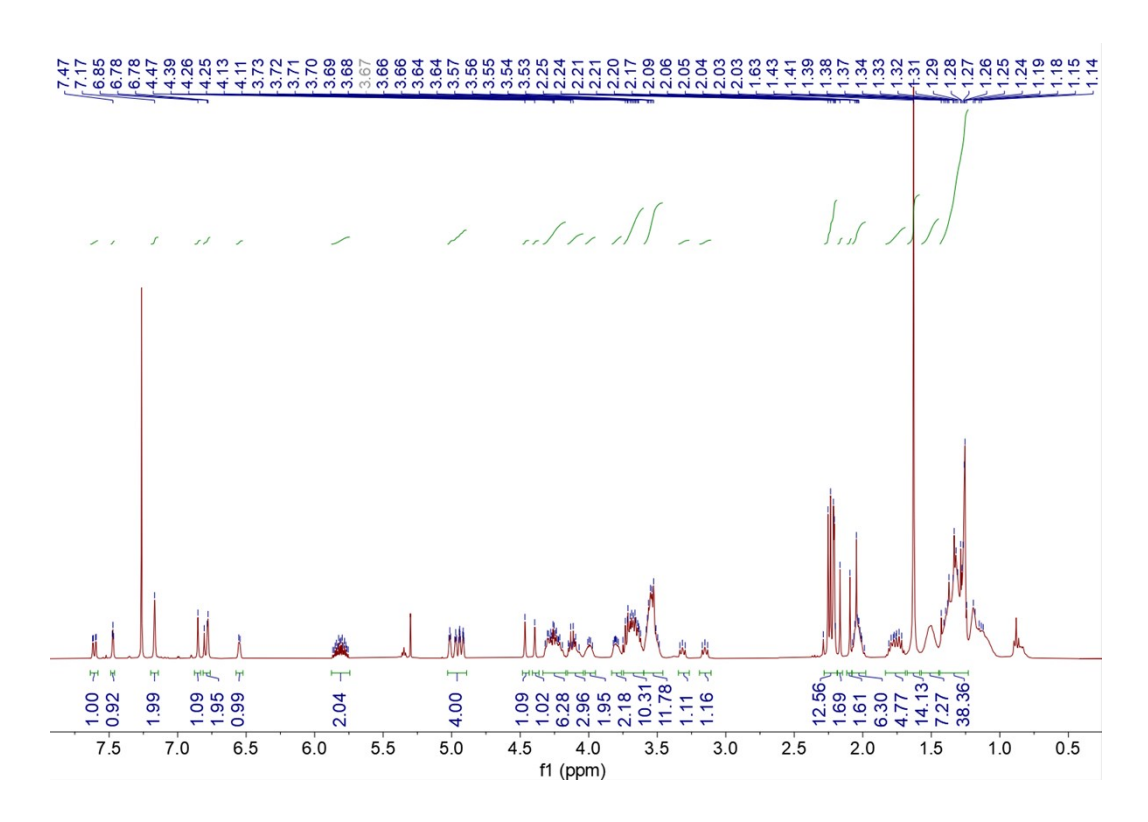


Figure S10. <sup>1</sup>H NMR spectrum (400 MHz, CDCl<sub>3</sub>, 298K) of monomer E.

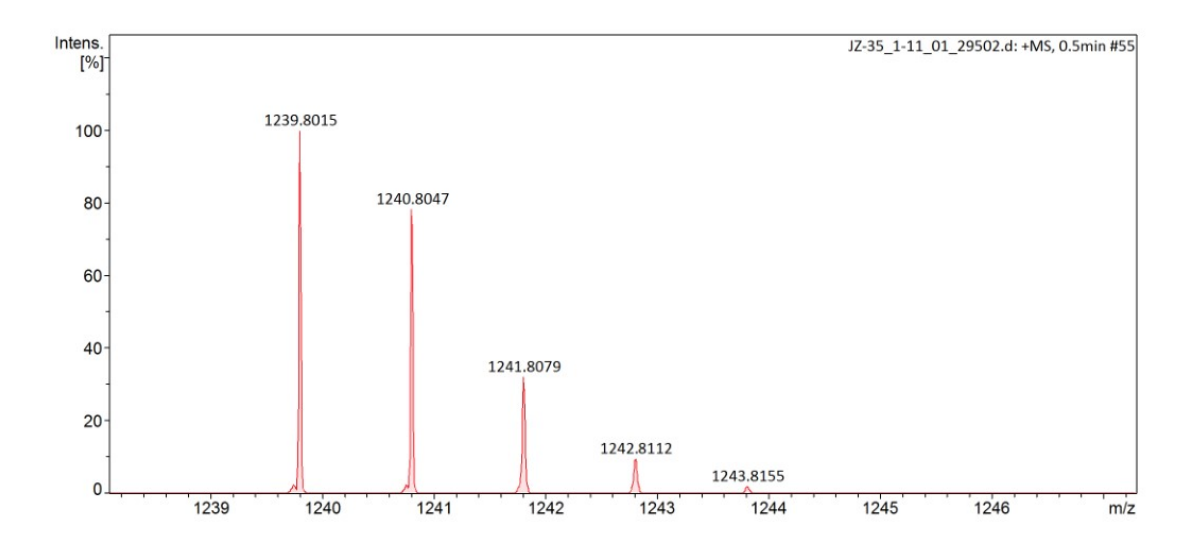


Figure S11. Electrospray ionization mass spectrum of monomer E.

# 4. Thermal stability characterization of PNs-1-3

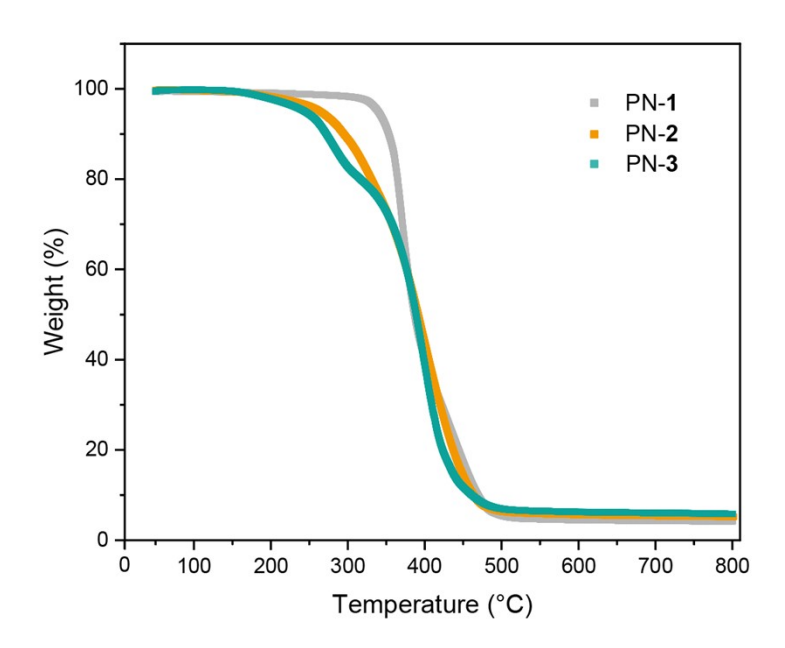
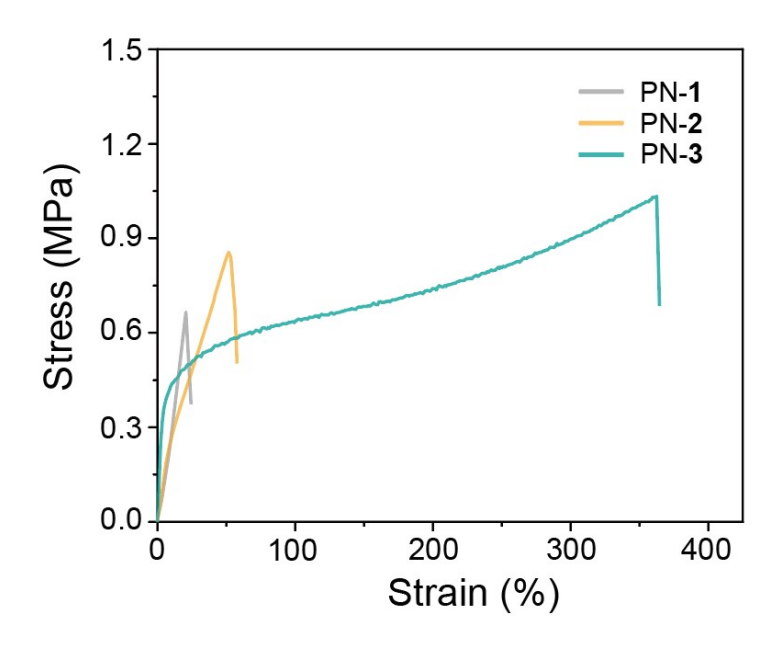


Figure S12. TGA curves of PN-1, PN-2 and PN-3 recorded under  $N_2$  flow (50 mL/min) with a heating rate of 20 °C/min.

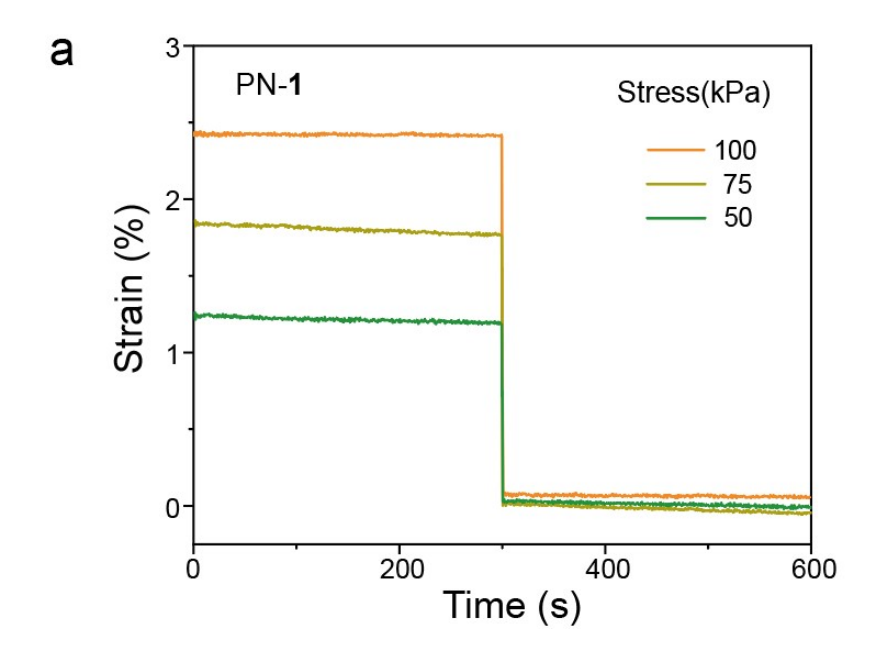
## 5. Tensile tests of PNs-1-3 under iso-frictional conditions



**Figure S13.** Stress-strain curves of PN-1, PN-2 and PN-3 at a temperature of 20 °C above their respective glass transition temperature ( $T_g$ ) values and recorded with a deformation rate of 100 mm/min.

To further demonstrate that  $T_g$  is not the primary influencing factor, we performed the tensile tests on PNs-1-3 under iso-frictional conditions, where the temperature was controlled to 20 °C above their respective  $T_g$  values. The results clearly show that the mechanical properties continue to follow the ideal trend—with fracture strain and fracture stress increasing significantly with higher mechanical bonds content—even when tested in a state where segmental mobility is normalized. This provides direct evidence that the enhancement mechanism is inherent to the mechanical bonds, rather than being dependent on the absolute value of  $T_g$ .

## 6. Creep-recovery tests of PNs-1-3



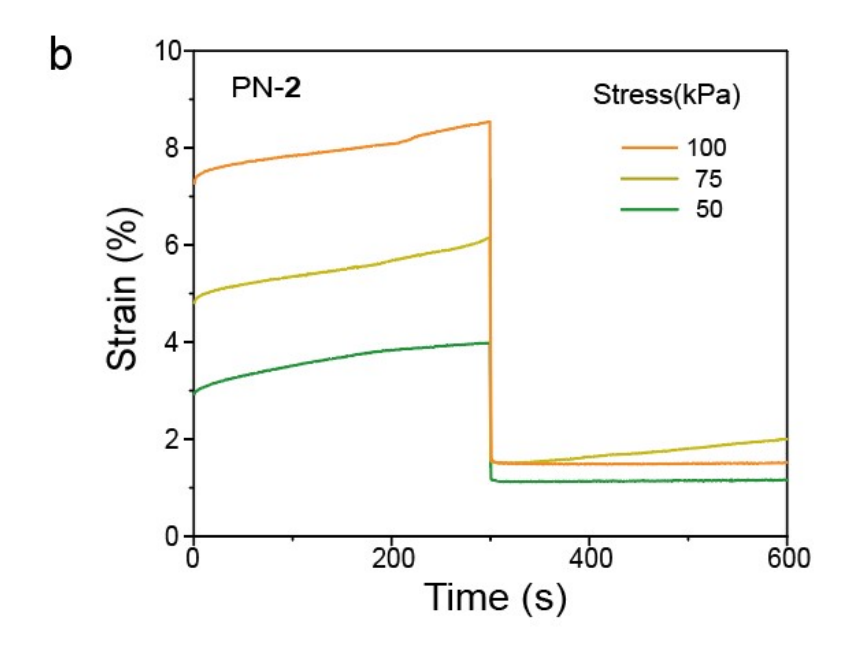




**Figure S14.** Creep-recovery curves of (a) PN-1, (b) PN-2 and (c) PN-3 under the stress of 100, 75, 50 kPa.

## 7. Characterization and mechanical tests of PNs-4-7

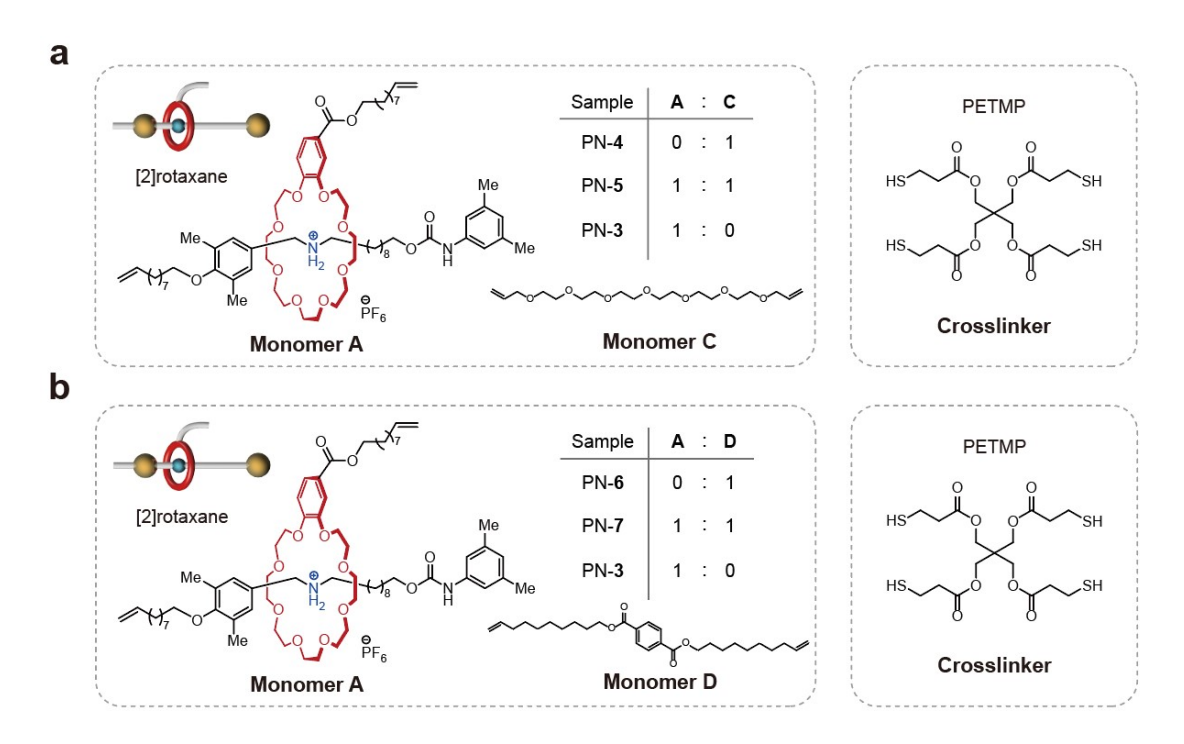


**Figure S15.** (a) Chemical structures and network formulations of monomer A, monomer C and crosslinker. (b) Chemical structures and network formulations of monomer A, monomer D and crosslinker.

We synthesized two types of new polymer networks using alternative monomers (denoted as monomer C and monomer D) that are significantly longer than monomer B. The objective of this experiment was to determine whether the dramatic enhancement in toughness and elongation observed in PN-3 (100% rotaxane) could be replicated simply by increasing monomer length.

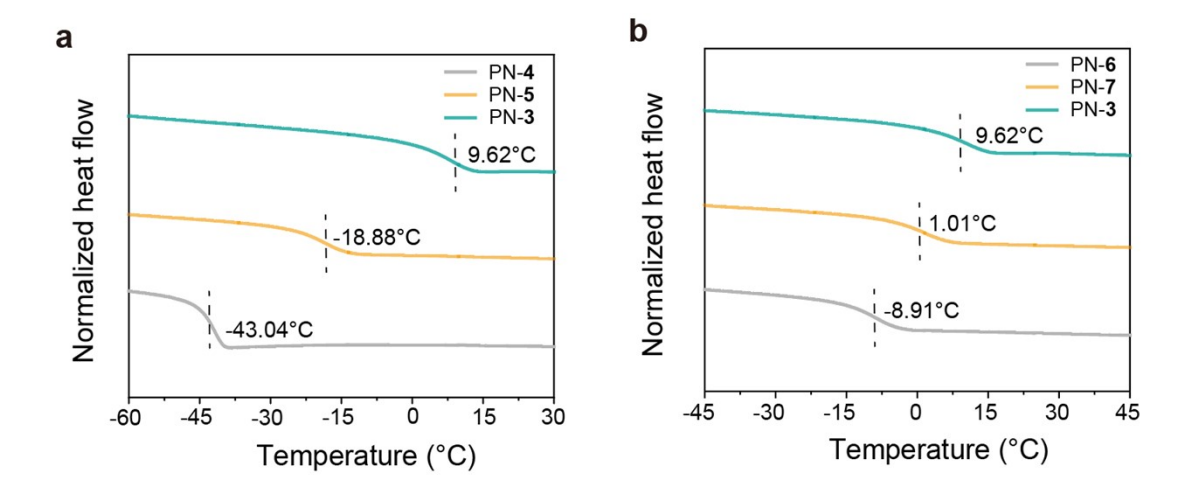


**Figure S16.** (a) DSC curves of PNs-4–5 (MINs based on monomer C) compared to PN-3, (b) DSC curves of PNs-6–7 (MINs based on monomer D) compared to PN-3, all measured by the second heating scan with a rate of 20 °C/min, showing different values of the glass transition temperatures.

The DSC curves reveal the  $T_g$  values from PN-4 to PN-7. Notably, comparing with the  $T_g$  values from PNs-1-3 (Fig. 2c), the  $T_g$  values also followed a descending sequence in accordance with the decreased mechanical bond density in the networks.

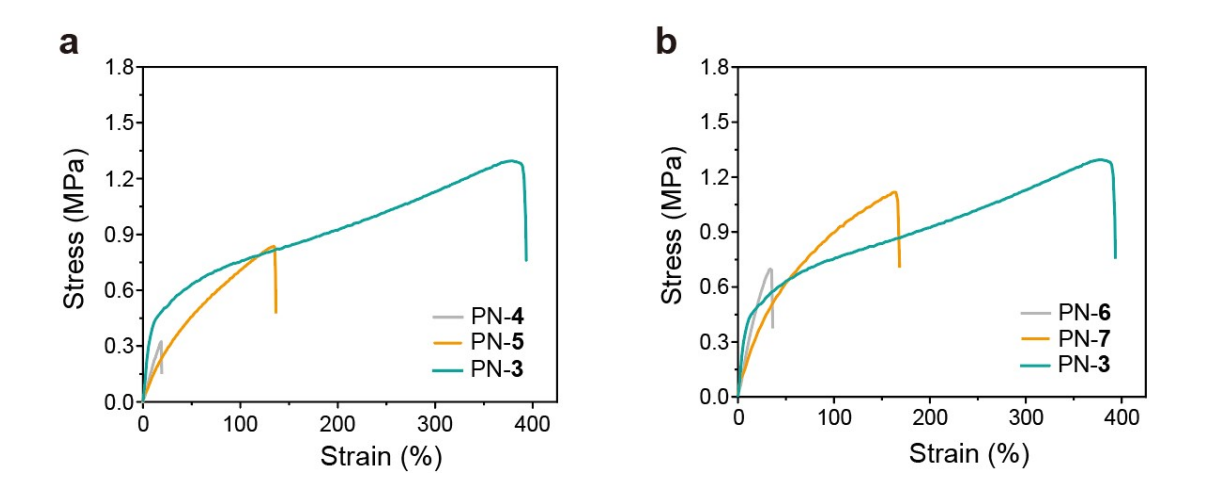


**Figure S17.** Stress—strain curves of (a) PN-3, PN-4, PN-5 and (b) PN-3, PN-6, PN-7 recorded with a deformation rate of 100 mm/min.

The curves demonstrate that merely increasing the monomer length did not result in a significant alteration of the mechanical property trends. The mechanical profiles for the networks PNs-4-5 and PNs-6-7, derived from the longer monomers, closely

cluster with those of the short-monomer networks from Fig. 3a in the main text and remain substantially inferior to the performance of PN-3.

#### 8. Characterization and mechanical tests of PNs-8-9

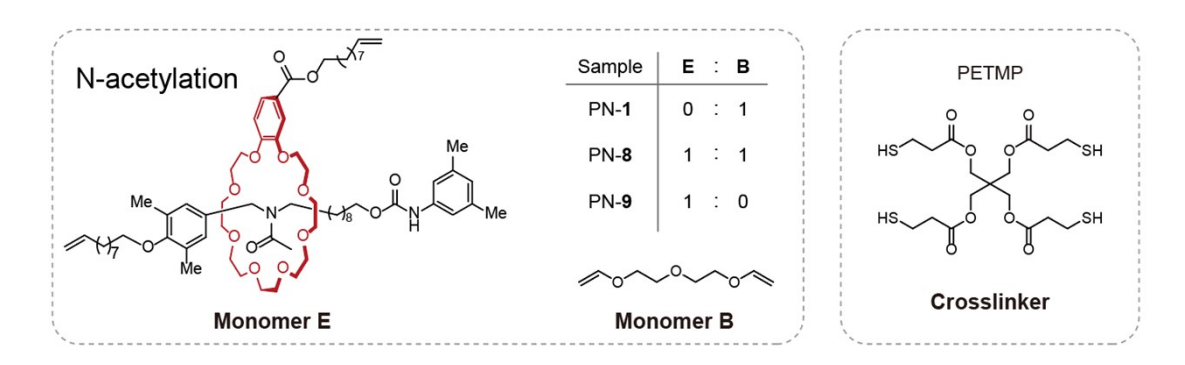


**Figure S18.** Chemical structures and network formulations of monomer E, monomer B and crosslinker.

To specifically isolate the effect of electrostatic interactions, we synthesized a charge-free analogue of the rotaxane monomer (monomer E). This was achieved via an acetylation reaction that effectively replaces the hexafluorophosphate recognition sites of secondary ammonium salt on the [2]rotaxane (monomer A), thereby eliminating the molecular charges while simultaneously removing the host–guest recognition capability. Thus, monomer E retains the identical mechanical bond and overall geometry but lacks the charged functional groups. As schematically illustrated, we progressively incorporated the charge-free monomer E into the polymer network, yielding two new samples: PN-8 (50% charge-free rotaxane) and PN-9 (100% charge-free rotaxane).

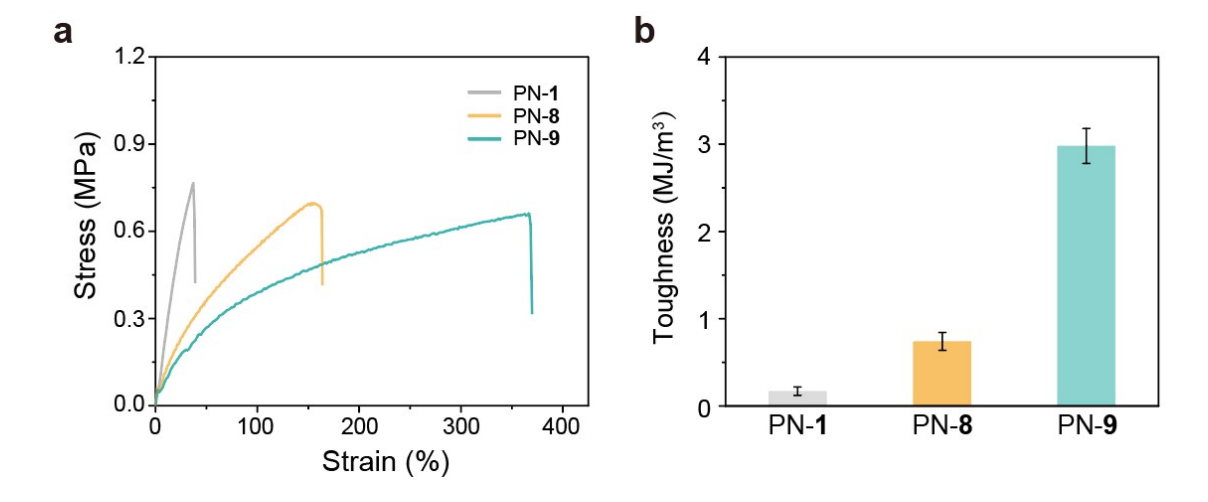
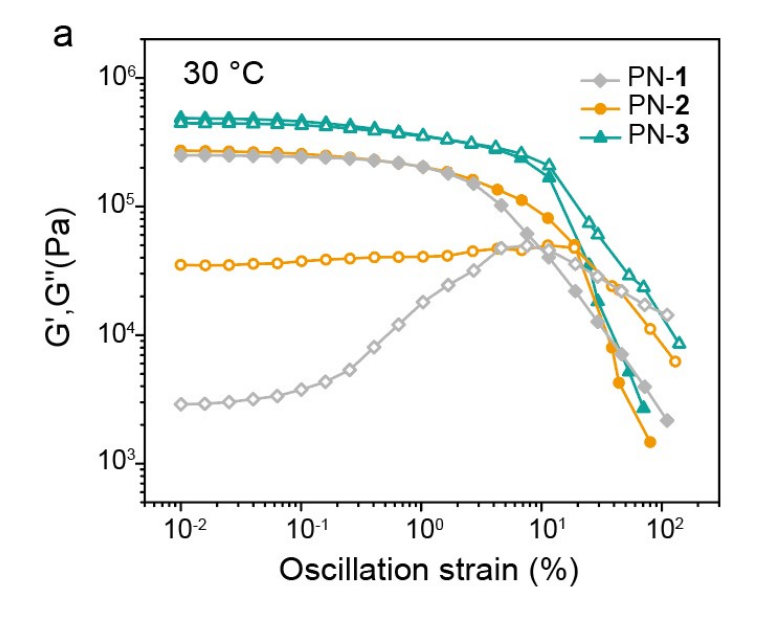


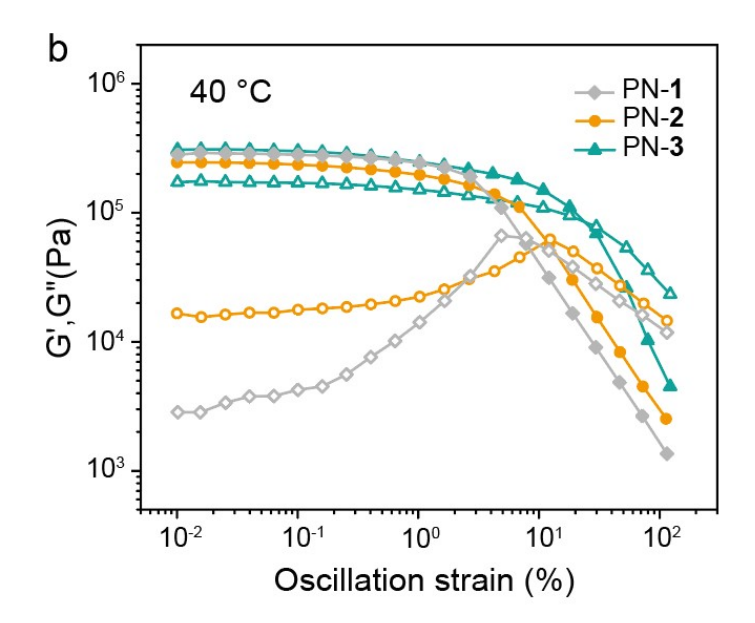
Figure S19. (a) Stress-strain curves of PN-1, PN-8 and PN-9 recorded with a

deformation rate of 100 mm/min. (b) Toughness of PN-1, PN-8 and PN-9 calculated from their stress-strain curves.

The tensile testing results of the charge-neutral networks shows that even after the complete removal of molecular charges, a substantial enhancement in fracture strain is still observed with increasing incorporation of the rotaxane. Furthermore, such improvement in extensibility is achieved without a concomitant sacrifice in fracture stress. Consequently, the calculated toughness, derived from the stress–strain curves, also shows a pronounced increasing trend. Firstly, PN-1 (0% charge-free rotaxane) exhibits a toughness of  $0.17 \pm 0.04$  MJ/m³, while PN-8 (50% charge-free rotaxane) shows a significantly enhanced toughness of  $0.74 \pm 0.09$  MJ/m³. Furthermore, toughness of PN-9 (100% charge-free rotaxane) achieves the highest value of  $2.98 \pm 0.28$  MJ/m³.

# 9. Rheological properties of different polymer networks





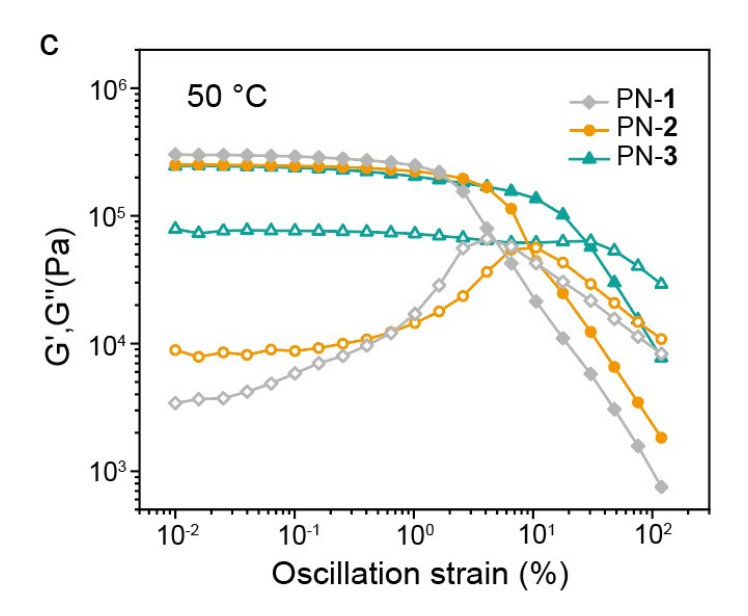


Figure S20. Strain sweep curves of PNs-1-3 at (a) 30, (b) 40 and (c) 50 °C.

The linear viscoelastic regions of the three networks can be obtained from the strain sweep curves in Fig. S20. As the strain increases further, the storage modulus (G') begin to decrease rapidly and the strain and stress of the system are no longer linearly related out of the region.

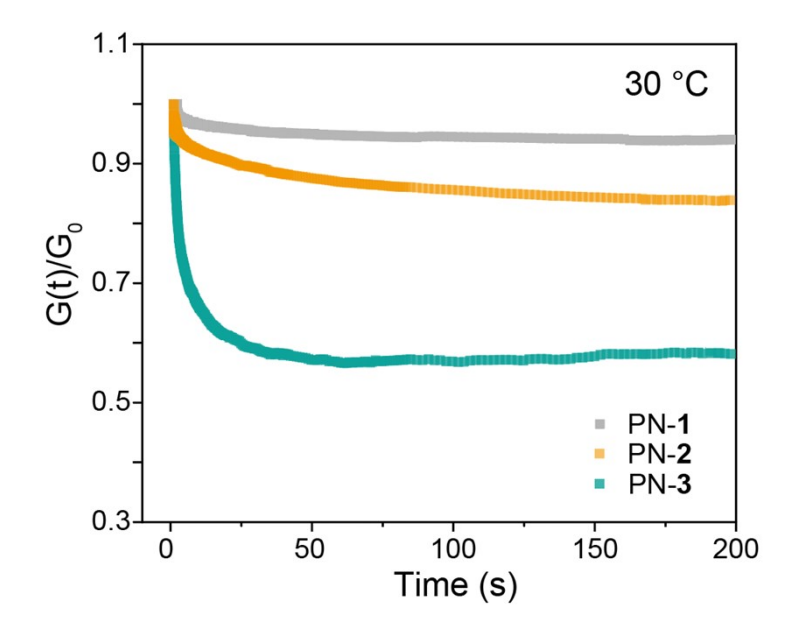
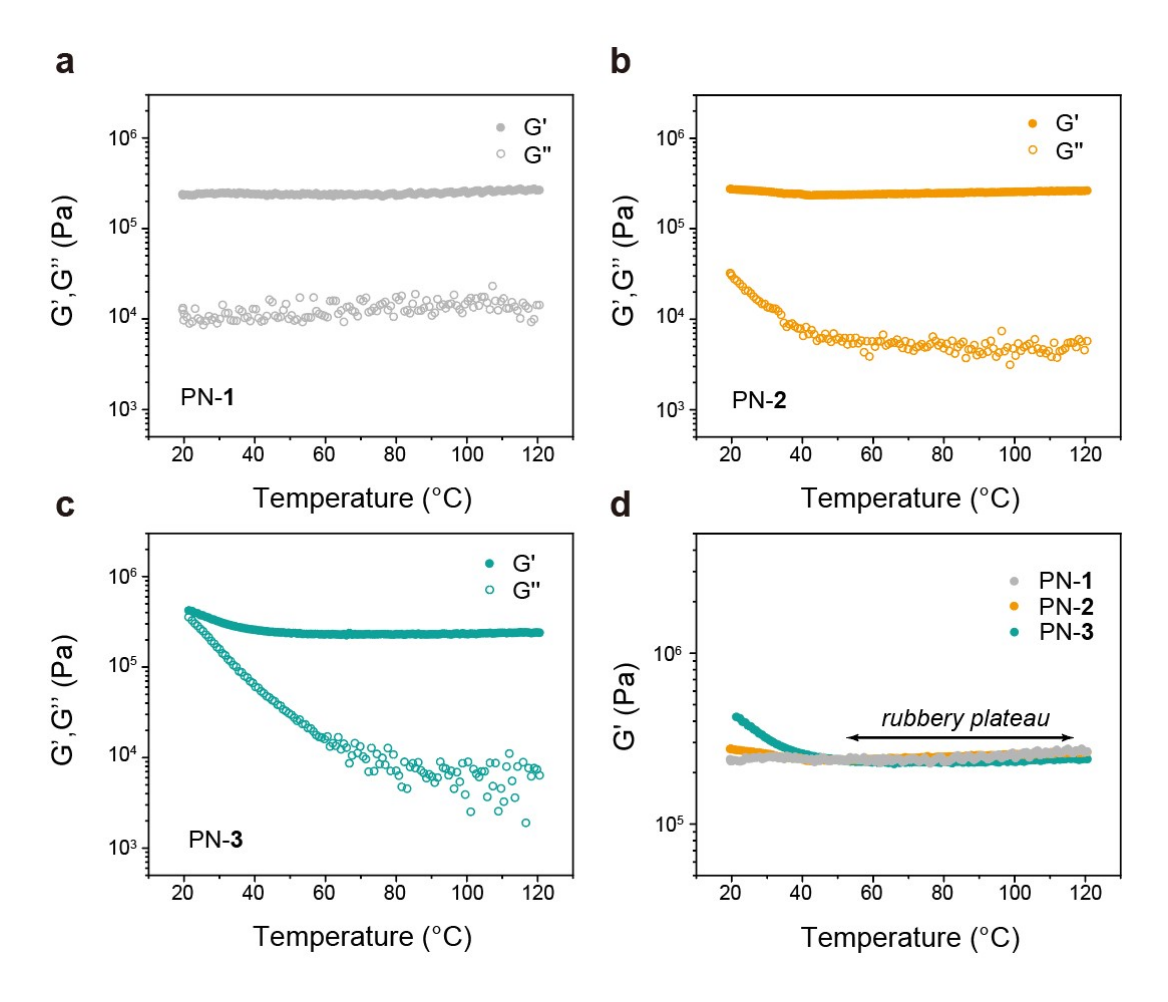


Figure S21. Stress relaxation experiments of PNs-1-3 at 30 °C.

Furthermore, stress relaxation experiments were performed on three networks under equivalent strain conditions in Fig. S21. Both the three samples displayed obvious relaxation behaviors, with an initial rapid relaxation phase followed by sustained residual stress. However, PN-3 showed the greatest capacity for residual stress release compared to PN-2 and PN-1. It could be contributed to the dissociation of host–guest recognition and the motion of mechanical bonds that drive to release dangling chains and relax stress efficiently. With the proportion of mechanical bonds increasing, the effect of relaxation improves accordingly.



**Figure S22.** Temperature sweep curves of (a) PN-1, (b) PN-2, and (c) PN-3 from 20 °C to 120 °C. (d) Rubbery plateau of PNs-1-3 obtained from the temperature sweep curves.

Based on the rubber elasticity theory to quantitatively calculate the crosslinking density (v), the equation is shown as below<sup>[3]</sup>:

$$v = \frac{E}{3RT} = \rho M_c^{-1}$$

Where R is the universal gas constant, E is the dynamic storage modulus of elastic plateau, T is the absolute temperature and  $\rho$  is the density of the polymer, while  $M_c$  is the molecular weight of the chain per cross-linked unit. Referring to this equation, the cross-linking density of different networks at specific modulus of the rubbery plateau can be well calculated.

Temperature sweeps were conducted on PNs-1-3. The results clearly showed a well-defined rubbery plateau for each network, confirming their crosslinked structure

and indicating stable thermomechanical behavior within the tested temperature range. Moreover, all three networks possess almost the same rubbery moduli, which means that their crosslinking densities are on the same level. Exhibiting a clear rubbery plateau after 50 °C, the crosslinking densities, calculated at 60 °C using the rubber elasticity theory above, were determined to be 28.53 mol/m³, 29.75 mol/m³ and 30.82 mol/m³ for PN-1, PN-2 and PN-3, respectively. These values are remarkably similar and show no statistically significant variation, strongly supporting the comparability of the three polymer networks.

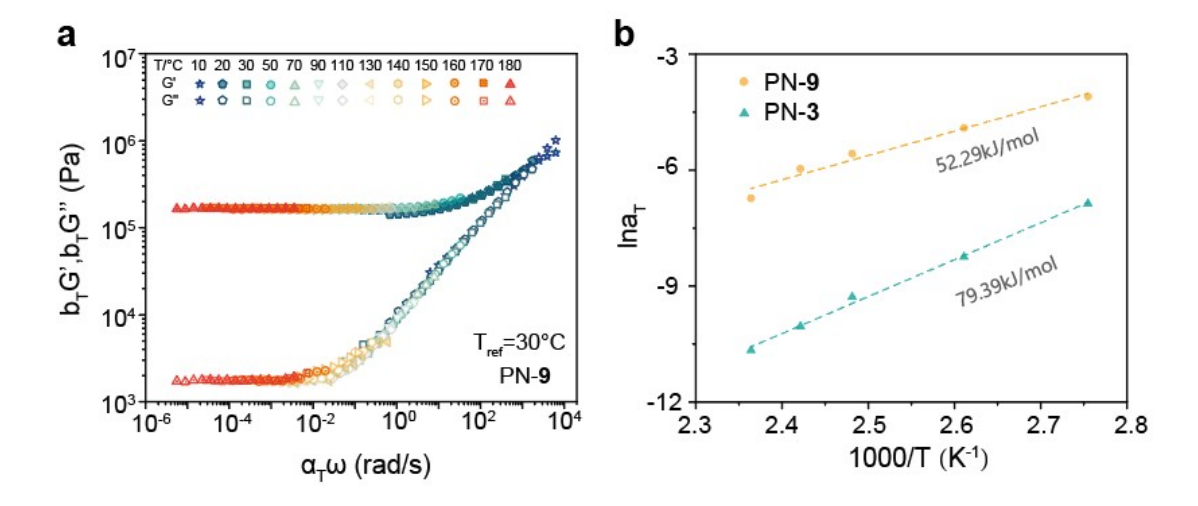


**Figure S23.** (a) Master curves of PN-9 at the reference temperature of 30 °C. (b) Fitting of  $\alpha_T$  for PN-3 and PN-9 to the Arrhenius equation at temperatures higher than 90 °C.

## References

- [1] L. Cheng, W. Wang, R. Bai, W.You, Y. Liang, Z. Yan, R. Zhang, X. Yan, W. Yu, *Angew. Chem. Int. Ed.*, 2025, **64**, e202422104.
- [2] X. Yang, W. Wang, R. Bai, Z. Guo, L. Cheng, Z. Zhang, W. Yu, X. Yan, *J. Am. Chem. Soc.*, 2025, **147**, 10540–10548.
- [3] P. J. Flory, *Principles of Polymer Chemistry*, Cornell University Press, New York, 1953, pp. 432–494.